Bio-impedance Simulation Platform using 3D Time-Varying Impedance Grid for Arterial Pulse Wave Modeling

Bassem Ibrahim*, Drew A. Hall†, and Roozbeh Jafari*

*Embedded Signal Processing (ESP) Lab, Texas A&M University, TX

†BioSensors and BioElectronics Group, University of California, San Diego, CA

bassem@tamu.edu, drewhall@ucsd.edu, rjafari@tamu.edu

Abstract—Accurate measurement of various parameters including the arrival time, velocity, and pressure of the arterial pulse wave is essential for continuous monitoring of hemodynamic parameters and early diagnosis of cardiovascular disease. Non-invasive sensors such as bio-impedance (Bio-Z) have been used to measure the arterial pulse wave by sensing the change in blood volume. However, the measured hemodynamic parameters are significantly affected by the electrode positioning relative to the artery and the electrode configuration. In this work, we created a Bio-Z simulation platform using a 3D time-varying impedance grid to model the arterial pulse wave. This platform can be used to guide design decisions (*i.e.* electrode placement relative to the artery and electrode configuration) prior to experimentation. We present simulations of the arterial pulse waveform for different sensor locations, current injection frequencies, and artery depths. The simulations are validated by measurements. This model will enable designers and researchers to create time-varying hemodynamic signals and rapidly test the effectiveness of circuits and algorithms without the need for extensive and burdensome experimentation.

Keywords— Bio-impedance, simulation, 3D tissue model

I. INTRODUCTION

Cardiovascular disease (CVD) is the leading cause of death worldwide; however, early detection is possible through continuous monitoring of hemodynamic parameters such as blood pressure (BP), pulse transit time (PTT), and heart rate (HR). Such cardiovascular parameters can be non-invasively derived from the morphology of the pressure pulse waveform measured by sensors such as bio-impedance (Bio-Z) where electrodes, for example placed on the wrist, estimate BP and PTT by monitoring the blood volume changes in the underlying blood vessels [1], [2]. Simple cardiac parameters such as HR can be measured from surface blood vessels such as capillaries and veins; however, complex cardiac parameters such as BP and PTT require accurate measurement from arteries – the deep, main blood vessels that carry the oxygenated blood from the heart to the rest of the body. Our objective is to introduce a simulation platform to guide designers measuring hemodynamic signals by modeling the propagation of the pressure pulse waveform from the arteries to the skin surface through the tissue and determine specifications of circuits and algorithm early without the need for extensive experimentation.

In prior work, photoplethysmogram (PPG) sensors were used to monitor the pressure pulse waveform for various
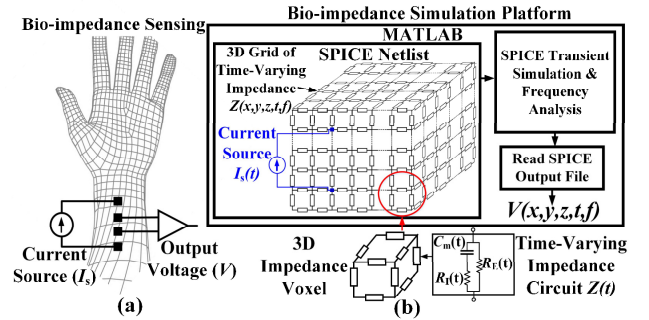

Fig. 1. Overview of (a) Bio-Z sensing and (b) 3D time-varying Bio-Z model.

applications such as measuring BP from a wrist-worn device [3]. The challenge with optical modalities is that light cannot travel deep into the tissue and can only capture blood volume changes near the skin surface (*i.e.* from capillaries). On the other hand, since Bio-Z injects a current, it can reach deeper tissue compared to the propagation depth of light used by PPG sensors. Thus, the Bio-Z signal provides a more accurate measurement of arterial blood volume changes since it can reach deep arterial sites. PPG is also affected by ambient light and skin tone, neither of which affects Bio-Z. Additionally, Bio-Z can be used for respiration and hydration measurements further increasing its utility. Previous work on Bio-Z modeling and simulation has limitations in that the models are static using constant impedances that do not capture the dynamic nature of the signal [4]. A 2D static finite element model using COMSOL for the artery pulsation was proposed in [5]. This method cannot provide time simulations for the arterial wave at different sensing locations relative to the artery.

In this paper, we propose a Bio-Z simulation platform based on a time-varying 3D impedance grid to model dynamic activity inside the body, as shown in Fig. 1. We model the body tissue using a 3D grid of small, interconnect, time-varying impedance elements (voxels). Each voxel consists of the equivalent circuit of cells within tissues. A parameterized SPICE model describes the geometry and conductivity of the modeled tissue, diameter, depth, and location of the arteries, and the location and spacing of the electrodes on the skin. The proposed model can be integrated with the sensing circuits in SPICE simulations using our source code, which is available online to help designers and researchers understand design decisions and tradeoffs [11].
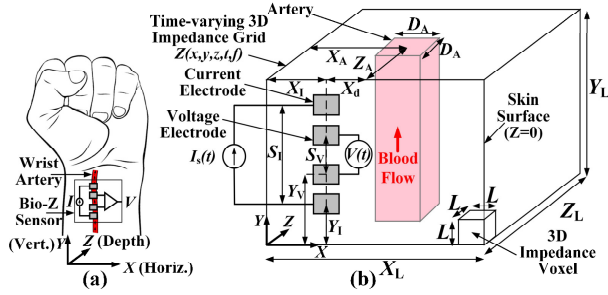
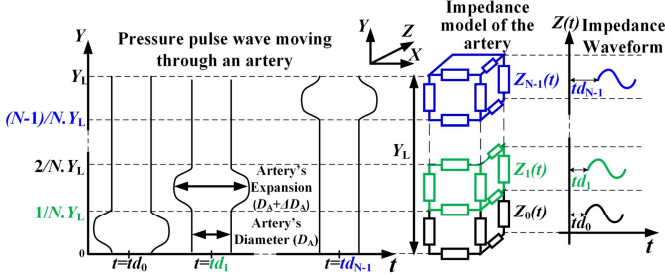Fig. 2. (a) Bio-Z sensing, (b) parameters of the 3D Bio-Z model.

Fig. 3. 3D model of an artery.

II. METHODS

A. 3D Bio-Z Model

Human tissue consists of cells that can be modeled as an electrical circuit by R_I, R_E and C_m, which represent the intra- and extra-cellular fluid resistance, and cell membrane capacitance, respectively, as shown in Fig. 1(b). Bio-Z is measured by injecting an AC current and measuring the resulting voltage difference using a separate pair of electrodes (4-probe Kelvin sensing), as shown in Fig. 2(a). The measured signal consists of a constant component, Z_{DC}, and a time-varying component, $\Delta Z(t)$, which corresponds to the blood volume change (and thus the pressure pulse waveform). To accurately model the tissue, we use an equivalent circuit model for every voxel to get high spatial resolution. Thus, this Bio-Z model consists of a large 3D hypercube of connected voxels mimicking the physiology of the body and vasculature. The impedance of each voxel consists of constant (*i.e.* fat and bones) and time-varying (*i.e.* blood vessels) components. In this paper, we present a 3D model for the wrist with an artery carrying blood in the vertical direction (Y-axis) assuming the skin surface is the $Z = 0$ plane where the electrodes are placed vertically parallel to the artery, as shown in Fig. 2(b). This model is highly parameterized where: L is the length of the impedance voxel; X_L, Y_L, and Z_L are the geometry of the body; Z_A, X_A, and D_A are the artery depth, location, and diameter; I_s is the amplitude of the current injection; X_I, Y_I, and S_I are the current electrode location and spacing ; and Y_V, and S_V are the voltage electrode location and spacing. This model is highly programmable and can be used to model any part of the body such as the chest where $\Delta Z(t)$ can be assigned to the heart and lung movements to simulate the impedance cardiogram and respiration rate.

B. 3D Model of the Artery

Each cardiac cycle, the heart pumps blood to the body which causes a pressure pulse to travel through the arteries. Parameters associated with the traveling pulse include the pulse arrival time, which is the time that the pulse arrives at a specific location, and

the PTT which is the time it takes for the pulse to travel between two points along the artery. The pulse pressure causes expansion of the artery's diameter from D_A to $D_A + \Delta D_A$ resulting in an increase of blood volume from v to $v + \Delta v$. The increase in blood volume Δv leads to a decrease in the extra- and intra-cellular fluid resistances, ΔR_E and ΔR_I, and an increase in the cellular membrane capacitance, ΔC_m. This change in impedance is modeled by a sinusoidal waveform with frequency f equal to the heart rate as in (1). Although many hemodynamic parameters can be modeled, we chose to model PTT in this paper due to its importance in estimating the blood pressure. To model PTT, each 3D impedance voxel along the artery is assigned a delay of td_i as a linear function of i as in (2) from $i = 0$ to $i = N - 1$, where i is the voxel index and N is the total number of voxels in the Y-direction, as shown in Fig. 3.

$$Z_i(t) = \begin{cases} R_I(t) = R_I - \Delta R_I \sin(2\pi f(t - td_i)) \\ R_E(t) = R_E - \Delta R_E \sin(2\pi f(t - td_i)) \\ C_m(t) = C_m + \Delta C_m \sin(2\pi f(t - td_i)) \end{cases} \quad (1)$$

$$td_i = \frac{i}{N} PTT \text{ for } i = 0 \text{ to } N - 1 \quad (2)$$

C. Simulation Flow

The Bio-Z simulation platform uses MATLAB to generate a SPICE netlist of the 3D grid of time-varying impedances $Z(x,y,z,t,f)$ and the current source $I_s(t)$ according to the model parameters as shown in Fig. 1(b). Then, MATLAB invokes LTSPICE to run the simulation with simulation options (*e.g.*, simulation time and time step for transient analysis or start and stop frequencies for frequency analysis). LTSPICE generates an output text file that contains the node voltages for each voxel. MATLAB reads this file and arranges the data in a multi-dimensional array, $V(x,y,z,t,f)$ for post-processing.

III. RESULTS

We selected the model parameters to represent the anatomy of the wrist. Specifically, we chose $D_A = 2.5$ mm and $Z_A = 3.5$ mm, which were the average values obtained from 44 subjects [6]. The ratio of the DC resistance of the blood and tissue was selected to be 4 to 7 [7]. In the simulation, we used $I_s = 1$ mA and $PTT = 10$ ms, similar to our experimental measurements of Bio-Z from the radial artery of the wrist. We estimated Z_{DC} and ΔZ by fitting the model output V_{DC} and ΔV to our experimental measurements. We choose $L = 1$ mm to balance spatial resolution and simulation complexity.

We validated the proposed framework by matching simulation results between the proposed model and finite element method (FEM) from EIDORS software that is implemented in MATLAB for electrical impedance tomography (EIT) [8]. We simulated a 2D Bio-Z model with a square shape surrounded by 40 electrodes uniformly distributed on the perimeter used for current injection and voltage sensing with 10 electrodes on each side, as shown in Fig. 4(a). The current was injected from each adjacent pair of electrodes and the voltage measured from all remaining electrodes for a total of 1480 (37×40) measurements. Fig. 4(b) and (c) show the variation of the output DC voltage V_{DC} versus electrode location with large peaks observed when the current and the voltage electrodes are at the closest distance from each other which occurred at the 4
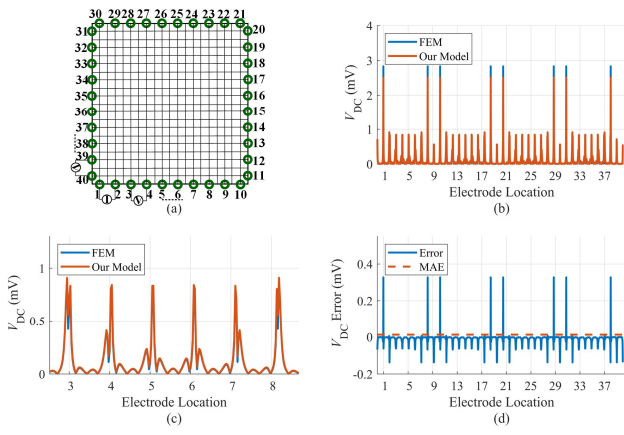
Fig. 4. Comparison between V_{DC} for EIT measurements from the proposed model and FEM: (a) electrodes configuration, (b) all EIT measurements, (c) subset of EIT measurements, and (d) proposed model error.
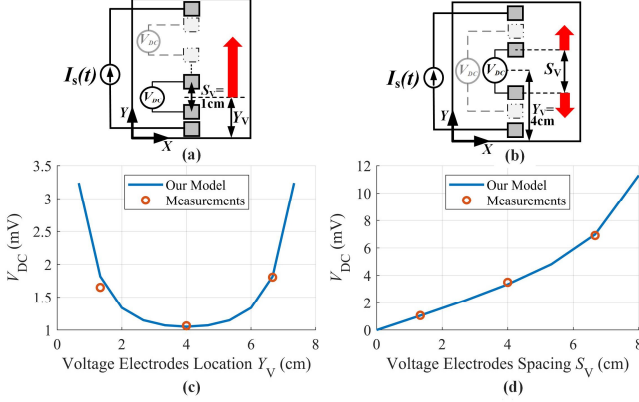

Fig. 5. Comparison between the simulated and measured V_{DC}: (a) and (c) versus voltage electrode location Y_V ($S_V = 1$ cm), (b) and (d) versus voltage electrode spacing S_V ($Y_V = 4$ cm).

corners of the square (*i.e.* 8 electrode locations: 1, 9, 11, 19, 21, 29, 31, and 39). The output voltage from the proposed model and conventional FEM were very close with a mean absolute error (MAE) of 10 µV, as shown in Fig. 4(d).

In addition, the proposed 3D model was validated versus experimental Bio-Z measurements collected from human subjects under Texas A&M University IRB (IRB2017-0086D) by the comparison of the DC voltage V_{DC}, voltage changes ΔV, and PTT for different model parameters. In the first experiment, we measured V_{DC} while changing the vertical location of the voltage electrodes Y_V between the current electrodes, as shown in Fig. 5(a). The measured V_{DC} was maximum when the voltage electrodes were closer to the current electrodes (minimum and maximum Y_V) and was minimum when the voltage electrodes were in the middle, as shown in Fig. 5(c). In another experiment, we measured V_{DC} with voltage electrodes placed in the middle between current electrodes for different voltage electrodes spacing S_V, as shown in Fig. 5(b). The measured V_{DC} increased with an increased spacing of the voltage electrodes S_V, as shown in Fig. 5(d). In these experiments, the simulation and measurement results were very close.

We studied the changes in the peak-to-peak amplitude of the time-varying component of the measured voltage, $\Delta V_{PP}(x,y)$, versus location across the X and Y directions between each pair of adjacent nodes of the grid at the skin surface ($Z = 0$) with the
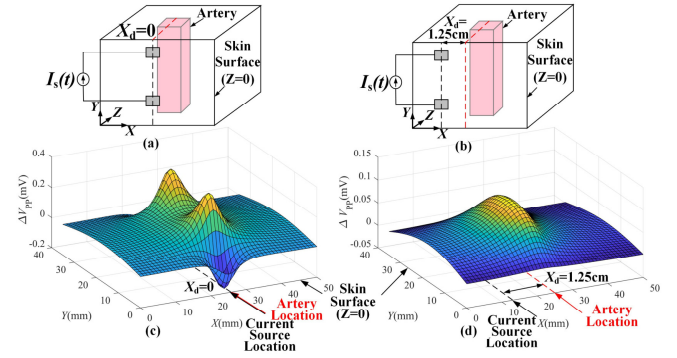

Fig. 6. ΔV_{PP} across the X and Y directions at the skin surface ($Z = 0$): (a) and (c) current electrodes placed on the artery ($X_d = 0$), (b) and (d) away from the artery ($X_d = 1.25$cm).
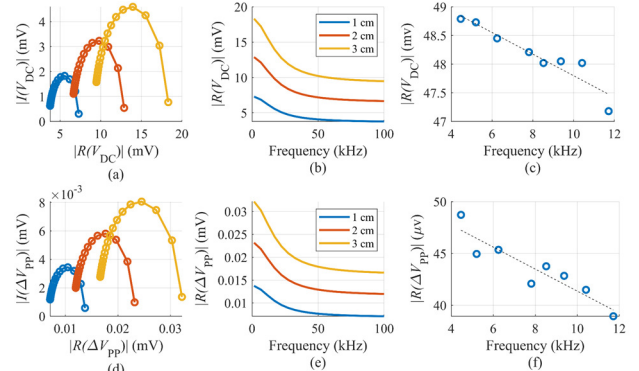

Fig. 7. Bio-Z frequency analysis: (a) and (b) simulations of V_{DC} for different voltage electrode spacing $S_V = 1$, 2 and 3cm, (c) measurements of V_{DC} (d) and (e) simulations of ΔV_{PP}, and (f) measurements of ΔV_{PP}.

distance between current electrodes and the artery $X_d = 0$ and 1.25 cm, as shown in the electrode configurations in Fig. 6(a) and (b). Fig. 6(c) shows ΔV_{PP} with an area of high amplitude centered around $X = 25$ mm, which is the location of the artery. The maximum amplitude of ΔV_{PP} decreased from 0.2 to 0.05 mV when X_d increased from 0 to 1.25 cm. We observed that the $\Delta V_{PP}(x,y)$ was modulated by the DC voltage $V_{DC}(x,y)$ generated from the current injection with peaks close to the location of the current electrode. These results show that the placement of voltage electrodes close to the artery and to the current electrodes is important to maximize the measured blood volume changes from the arteries, which leads to a better estimation of hemodynamic parameters.

We also performed a Bio-Z frequency analysis of the proposed model using SPICE simulation (.ac mode). Fig. 7(a) and (b) show the magnitude of the real and imaginary components of V_{DC} ($|R(V_{DC})|$ and $|I(V_{DC})|$) versus frequency, which are similar to the theoretical Cole-Cole plot. Both $|R(V_{DC})|$ and $|I(V_{DC})|$ increased as the distance between the electrodes increased from 1 to 3 cm, like the experimental measurements in our previous study [9]. The behavior of ΔV_{PP} versus frequency was similar to V_{DC}, as shown in Fig. 7(d) and (e). This matched our measurements of $|R(V_{DC})|$ and $|R(\Delta V_{PP})|$ from the radial artery on the wrist over the frequency range of 4 to 12 kHz, as presented in Fig. 7(c) and (f). Both DC and peak-to-peak amplitudes decreased as the frequency increased with a correlation coefficient of 0.89.
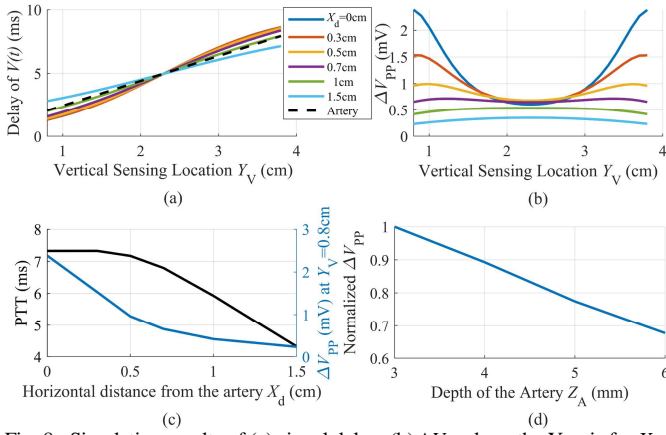
Fig. 8. Simulation results of (a) signal delay, (b) ΔV_{PP} along the Y-axis for X_d from 0 to 1.5 cm, (c) PTT and ΔV_{PP} versus X_d with current electrodes at $Y = 0.8$ and 4.6 cm and $S_V = 0.8$ cm and (d) ΔV_{PP} versus artery's depth Z_A.

We used the proposed model to simulate the PTT as the difference in the delay between two vertical sensors at different horizontal distances relative to the artery (X_d). We used an electrode configuration similar to Fig. 5(a) while varying the voltage electrode location Y_V with fixed current electrodes at $Y = 0.8$ and 4.6 cm, $S_V = 0.8$ cm, and an artery with PTT = 10 ms. Fig. 8(a) shows the delay of the voltage signal $V(t)$ representing the arrival time of the pulse wave versus the vertical sensing location Y_V. The delay increased in a non-linear function along the Y-axis in the same direction of the pressure pulse wave that was used in the proposed model. We repeated this simulation for various distances (X_d) between the sensing location and the artery ($X_d = 0$ to 1.5 cm). The slope of the delay with Y-axis decreased as X_d increased because the tissue has an averaging effect over a vertical distance on the artery that increases as the sensing location moves further from the artery. Consequently, at a very large distance from the artery, the delay will be constant along Y-axis with a value equal to the average of td_i of all the impedance voxels between the current electrodes. Fig. 8(b) shows the decrease of ΔV_{PP} with the increase of the distance from the artery. ΔV_{PP} has high peaks near the current electrodes when $X_d = 0$ as was shown previously in Fig. 6 and becomes flat as X_d increased because of the averaging effect of the tissue. We calculated the PTT as the difference between the minimum and maximum delay. Fig. 8(c) demonstrates the decrease of PTT and ΔV_{PP} with the increase of X_d. The simulated trends of PTT and ΔV_{PP} with X_d were validated with our previous Bio-Z measurements from 5 subjects from two vertical sensors on the radial artery on the wrist with $X_d = 0$ and 1.5 cm [10]. Table I shows the mean and standard deviation (STD) of the Bio-Z measurements over 5 minutes per subject. The measured subjects' mean PTT decreased from 6.8 to 3.0 ms and the mean

TABLE I
PTT AND AMPLITUDE MEASUREMENTS WITH $X_d = 0$ AND $X_d = 1.5$ CM

	X_d	Subj.	1	2	3	4	5	Mean
PTT (ms)	0	Mean	8.0	3.0	6.8	8.2	7.9	6.8
		STD	3.8	2.7	1.8	3.0	4.3	3.1
	1.5	Mean	3.4	-2.6	11.1	5.6	-2.5	3.0
		STD	7.0	4.9	2.9	5.2	7.9	5.6
ΔV_{PP} (μV)	0	Mean	33.1	33.9	56	52.4	27.4	40.6
		STD	10.1	5.8	6.2	10.2	5.5	7.5
	1.5	Mean	26.3	19.9	32.6	26.1	22.3	25.4
		STD	7.5	2.9	3.0	5.7	4.5	4.7

ΔV_{PP} decreased from 40.6 to 25.4 μV when X_d increased from 0 to 1.5 cm, which support our simulation results.

Finally, we used the proposed model to quantify the depth of penetration of the Bio-Z signal into the tissue to reach the artery. ΔV_{PP} at the surface was measured while changing the artery's depth Z_A from 3 to 6 mm. The normalized ΔV_{PP} decreased by only 32% when the artery's depth was doubled from 3 to 6 mm, as shown in Fig. 8(d). This demonstrates that Bio-Z is also suitable to detect pressure pulse waveform and hemodynamic parameters for individuals with high body mass index (BMI) and a thicker fat layer under the skin.

IV. CONCLUSIONS

In this paper, we presented a Bio-Z simulation platform using the proposed 3D grid of the time-varying impedance voxels to model the pulse wave in the arteries. We showed that modeling can estimate the behavior of pulse transit time and signal amplitude for different sensing locations relative to the artery. The proposed simulation platform was used to quantify the penetration of the bio-impedance signals inside the tissue for different arterial depths. Our simulation results were validated by experimental measurements. The proposed simulation platform can serve as an important tool to understand the propagation of pulse wave in the tissue and to improve Bio-Z sensing methods for measuring hemodynamic parameters and guide circuit designers and algorithm developers.

REFERENCES

[1] B. Ibrahim and R. Jafari, "Continuous blood pressure monitoring using wrist-worn bio-impedance sensors with wet electrodes," *IEEE Biomedical Circuits and Systems Conference (BioCAS)*, 2018.

[2] B. Ibrahim, A. Akbari, and R. Jafari, "A novel method for pulse transit time estimation using wrist bio-impedance sensing based on a regression model," *IEEE Biomedical Circuits and Systems Conference (BioCAS)*, 2017.

[3] S. Thomas, et al., "Biowatch: A noninvasive wrist-based blood pressure monitor that incorporates training techniques for posture and subject variability," *IEEE Journal of Biomedical and Health Informatics*, vol. 20, no. 5, pp. 1291–1300, 2015.

[4] A Morimoto, et al., "Spatial resolution in the electrical impedance tomography for the local tissue," *IEEE Engineering in Medicine and Biology 27th Annual Conference*, pp. 6638–6641, 2006.

[5] R. Mohamed, M. El Dosoky, and M. El-Wakad, "The effect of heart pulsatile on the measurement of artery bioimpedance," *Journal of Electrical Bioimpedance*, vol. 8, no. 1, pp. 101–106, 2017.

[6] J. Kim, Y. Lee, J. Lee and J. Kim, "Differences in the properties of the radial artery between cun, guan, chi, and nearby segments using ultrasonographic imaging: a pilot study on arterial depth, diameter, and blood flow," *Evidence-Based Complementary and Alternative Medicine*, 2015.

[7] G. Anand, A. Lowe, and A. M. Al-Jumaily, "Simulation of impedance measurements at human forearm within 1 kHz to 2 MHz," *Journal of Electrical Bioimpedance*, vol. 7, no. 1, pp. 20–27, 2016.

[8] M. Vauhkonen, et al., "A matlab package for the EIDORS project to reconstruct two-dimensional EIT images," *Physiological Measurement*, vol. 22, no. 1, pp. 107, 2001.

[9] B. Ibrahim, D. A. Hall, and R. Jafari, "Bio-impedance spectroscopy (BIS) measurement system for wearable devices," *IEEE Biomedical Circuits and Systems Conference (BioCAS)*, 2017.

[10] B. Ibrahim, D. Mrugala, and R. Jafari, "Effects of bioimpedance sensor placement relative to the arterial sites for capturing hemodynamic parameters," *IEEE Engineering in Medicine and Biology Society (EMBC)*, 2019.

[11] B. Ibrahim, D. A. Hall, and R. Jafari, "BioZPulse Simulation Platform", [Source Code]. http://www.github.com/TAMU-ESP/BioZPulse-Sim-Platform.